Supplementary Information

The glycerol stabilized calcium phosphate cluster for rapid remineralization of tooth enamel by a water-triggered transformation

Nan Luo[1,2#], Bing-Qiang Lu[3#*], Yu-Wei Deng[2,4], Hua Zeng[3], Yu Zhang[1,2], Jing-Yu Zhan[1,2], Xiao-Chen Xu[1,2], Gui-Zhi Cao[2], Jin Wen[2,4], Zhiyuan Zhang[2,5], Xi-Ping Feng[1,2], Xinquan Jiang[2,4], Feng Chen[3,6*], Xi Chen[1,2*]

Affiliations

[1]: Department of Preventive Dentistry, Shanghai Ninth People's Hospital, Shanghai Jiao Tong University School of Medicine, Shanghai, 200011, P. R. China

[2]: College of Stomatology, Shanghai Jiao Tong University; National Center for Stomatology; National Clinical Research Center for Oral Diseases; Shanghai Key Laboratory of Stomatology, Shanghai Research Institute of Stomatology, Shanghai, 200011, P. R. China

[3]: Center for Orthopedic Science and Translational Medicine, Department of Orthopedic, Spinal Pain Research Institute, Shanghai Tenth People's Hospital, School of Medicine, Tongji University, Shanghai, 200072, P. R. China

[4]: Department of Prosthodontics, Shanghai Ninth People's Hospital, Shanghai Jiao Tong University School of Medicine; Shanghai Engineering Research Center of Advanced Dental Technology and Materials, Shanghai, 200011, P. R. China

[5]: Department of Oral and Maxillofacial-Head Neck Oncology, Shanghai Ninth People's Hospital, Shanghai Jiao Tong University School of Medicine, Shanghai, 200011, P. R. China

[6]: Shanghai Key Laboratory of Craniomaxillofacial Development and Diseases, Stomatological Hospital and School of Stomatology, Fudan University, Shanghai, 200001 P. R. China

[#]: These authors contributed equally.

Corresponding Authors

*E-mail: bqlu@tongji.edu.cn

*E-mail: chen_feng@fudan.edu.cn

*E-mail: cherry_cxnet@sjtu.edu.cn

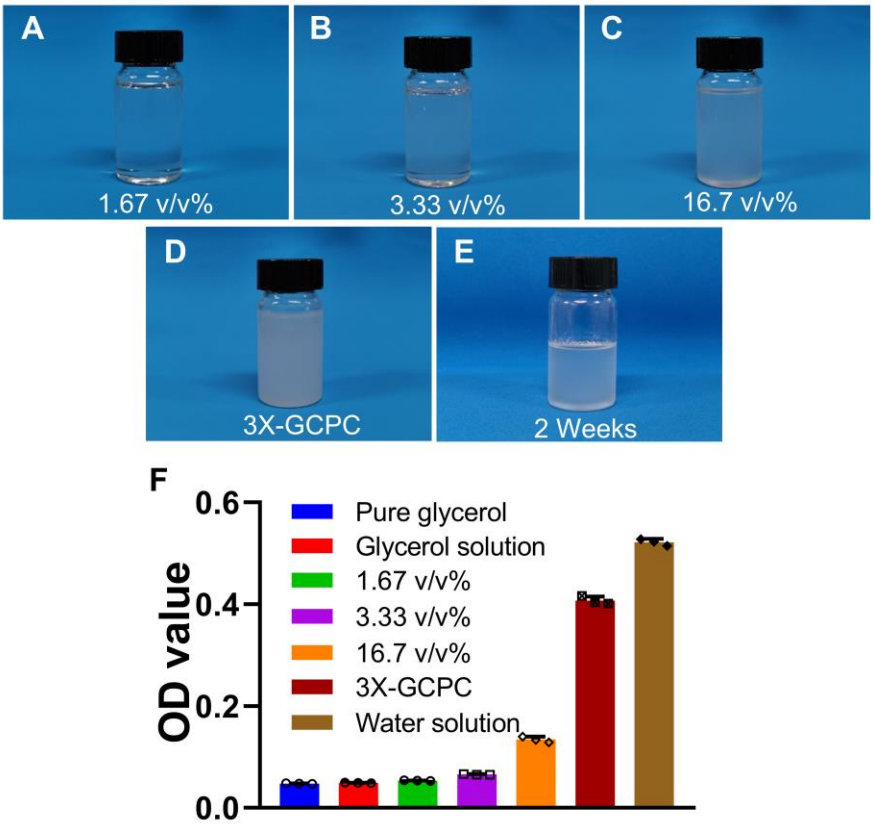

Supplementary Fig. 1. Appearances of the different solutions. (A-E) Digital images of the solutions with glycerol-dominant solvents. (F) Relative quantification of turbidity (OD value) of the samples. Pure glycerol represents glycerol solvent without dissolving the ions. Each of the other samples contains 1.00 mmol of Na_3PO_4 and 1.50 mmol $CaCl_2$, while 3X-GCPC triples the concentrations. Labels 1.67 v/v%, 3.33 v/v%, 16.7 v/v% represent GCPC prepared in the solutions with different water contents as indicated, and those of glycerol solution, 3X-GCPC and water solution have water content 0 v/v%, 16.7 v/v% and 100 v/v%, respectively. OD values are recorded at wavelength of 590 nm. Data are means ± standard deviations (n = 3 independent experiments).

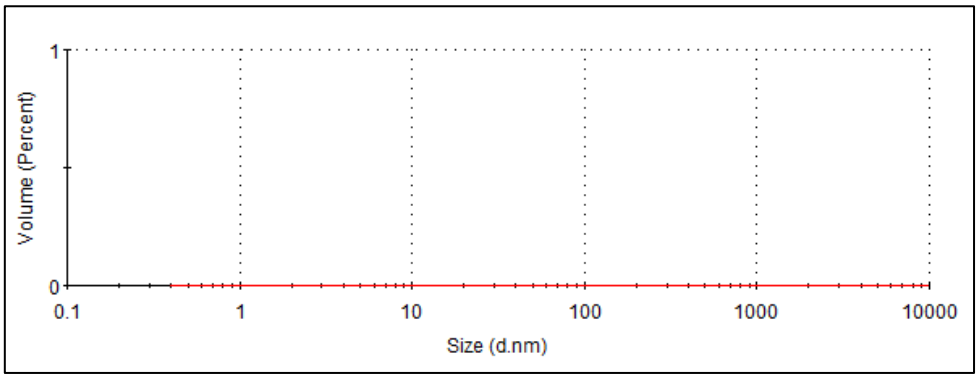

Supplementary Fig. 2. DLS analysis of the solution containing 0.033 mol/L PO_4^{3-} and 0.050 mol/L Ca^{2+} ions in glycerol solvent.

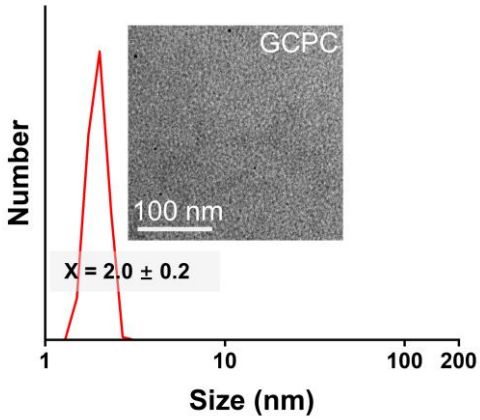

Supplementary Fig. 3. DLS analysis with the inset of TEM image of GCPC in glycerol-dominant solvent.

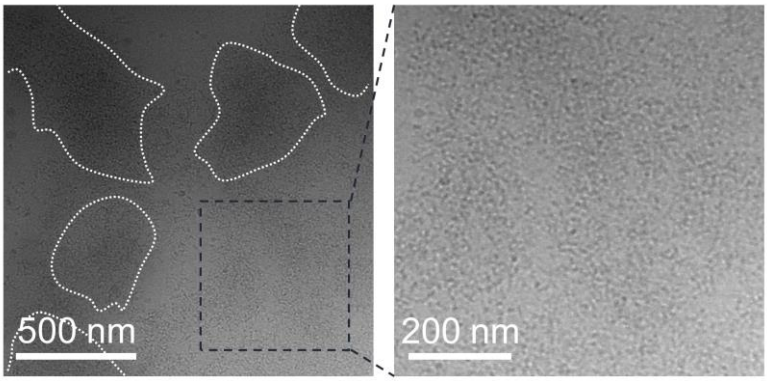

Supplementary Fig. 4. Liquid cell-ACTEM images of GCPC solution after storage at room temperature for 2 weeks. The white dotted lines outline the cluster-concentrated areas.

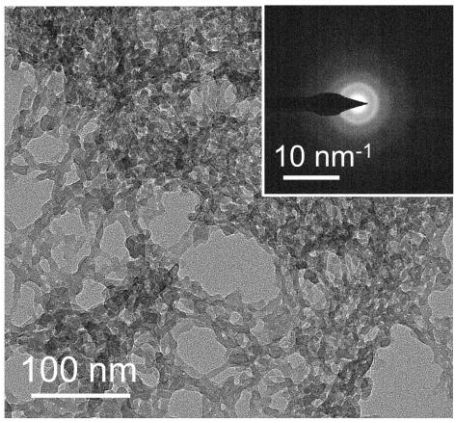

Supplementary Fig. 5. TEM image of the ACP nanoparticles obtained by mixing GCPC solution with water at a volume ratio of 1:10 (1 mL GCPC in 10 mL water). Inset: SAED pattern of the ACP nanoparticles.

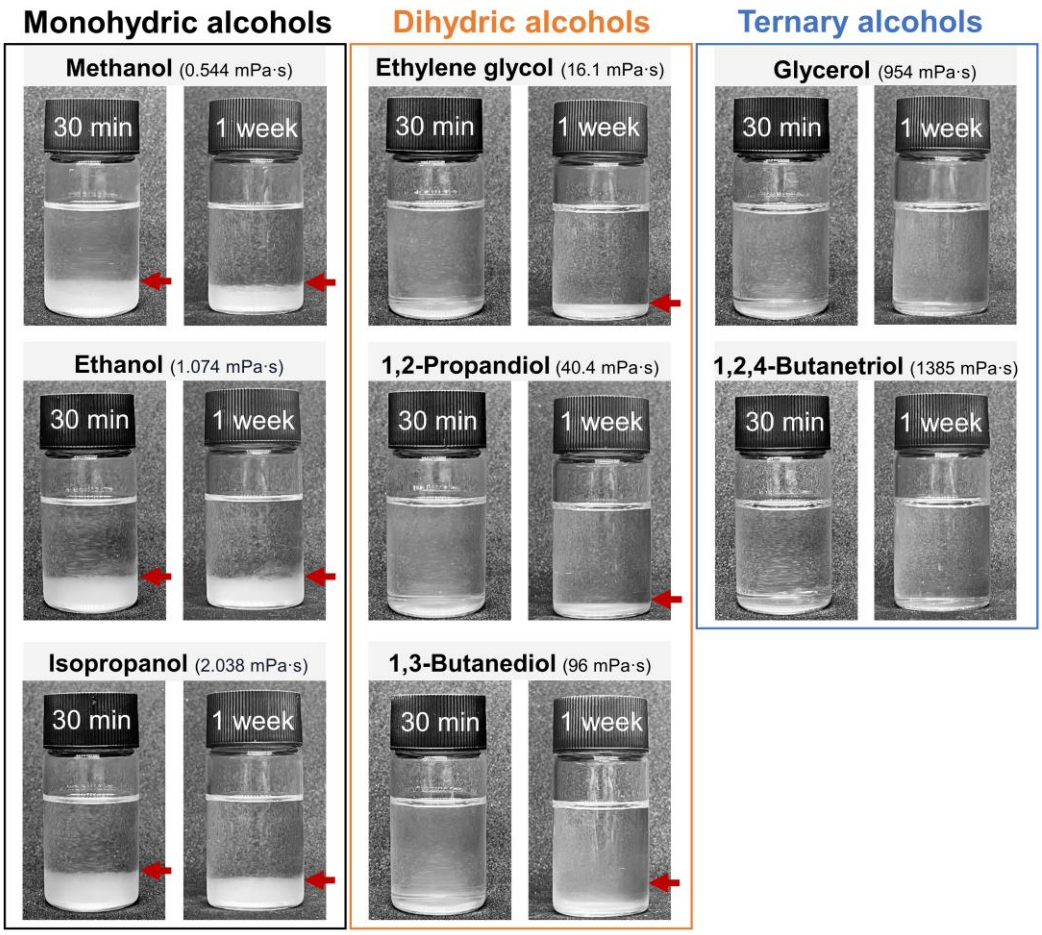

Supplementary Fig. 6. Photographs of different alcohols with varied viscosity mixed with GCPC in a volume ratio of 10:1 after 30 min and 1 week. Viscosity of each solvent at room temperature (25 ºC) is displayed beside its name. The red arrows mark the boundary between the visible precipitate and the transparent liquid.

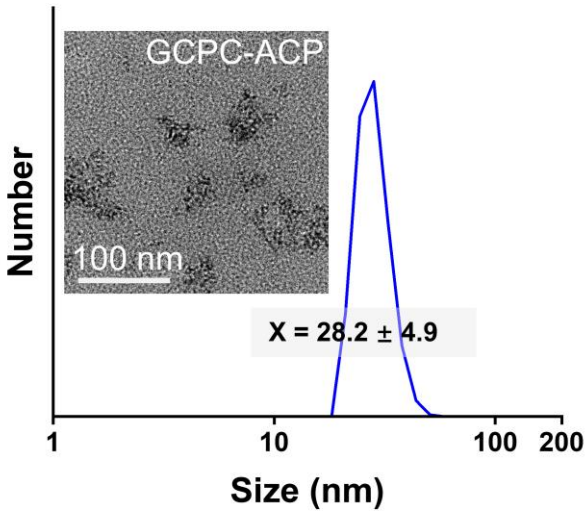

Supplementary Fig. 7. DLS analysis with the inset of TEM image of GCPC-ACP.

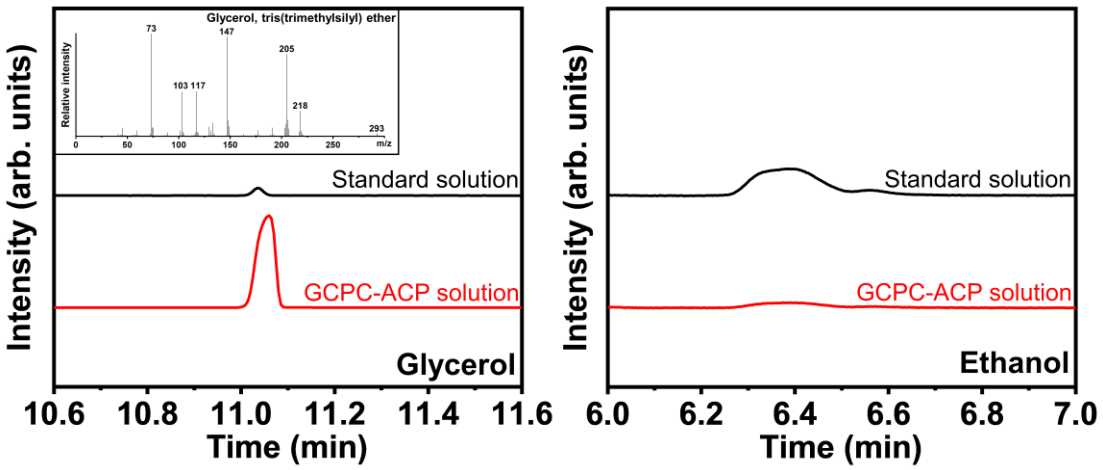

Supplementary Fig. 8. Analysis of glycerol and ethanol in GCPC-ACP. The GCPC-ACP extracted solutions were analyzed using GC-MS (left) and GC (right) to determine the content of glycerol (left) and ethanol (right) in it. Inset: mass spectrums of trimethylsilyl ether of glycerol derived from glycerol in GCPC-ACP extracted solution.

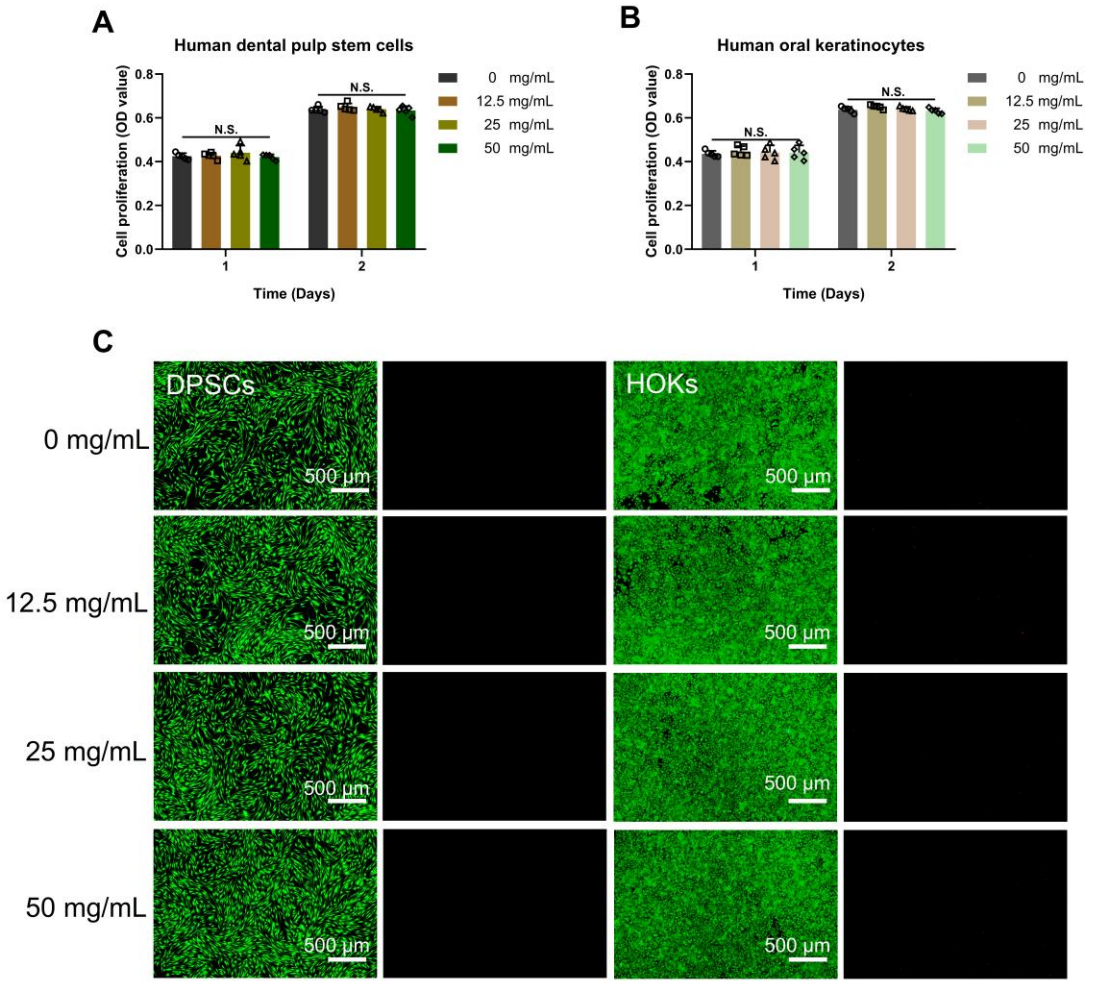

Supplementary Fig. 9. Cytotoxicity of GCPC. (A, B) CCK-8 assay of DPSCs (A) and HOKs (B). There are no significant differences of the cell proliferations between GCPC groups (12.5 mg/L, 25 mg/L, 50 mg/L) and control group (without GCPC or other materials, labeled 0 mg/L) after 1 d and 2 d. The error bars in (A) and (B) represent the mean ± SD for n = 5 independent experiments. N.S. indicates that there is no significant difference. (C) Live/dead staining of DPSCs and HOKs. Green fluorescence represents live cells and red fluorescence is related to dead cells.

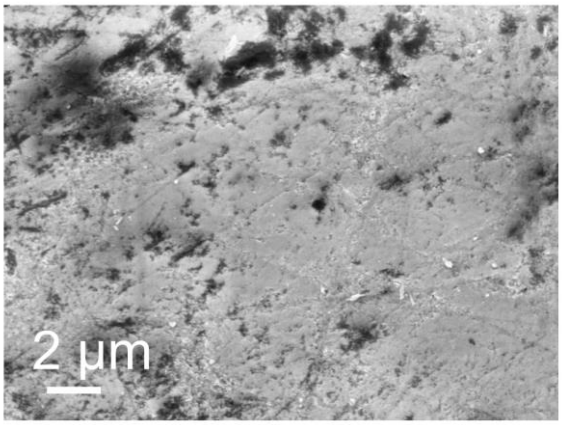

Supplementary Fig. 10. SEM image of the sound enamel without acid etching.

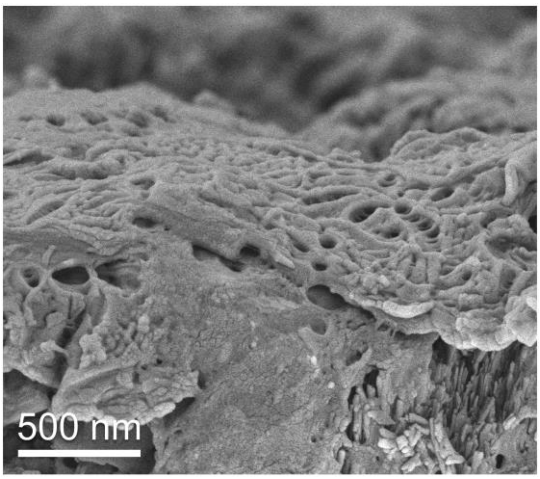

Supplementary Fig. 11. The cross-sectional view of the ACP nanowires formed on the acid etched enamel at 5 min.

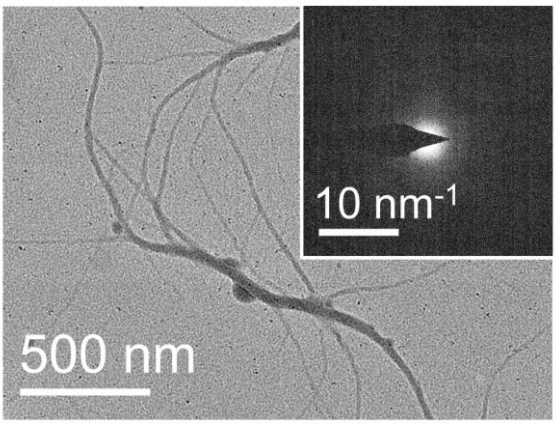

Supplementary Fig. 12. TEM image of nanowires formed by GCPC transformation on acid etched enamel surface at 5 min. Inset: corresponding SAED pattern of the nanowires.

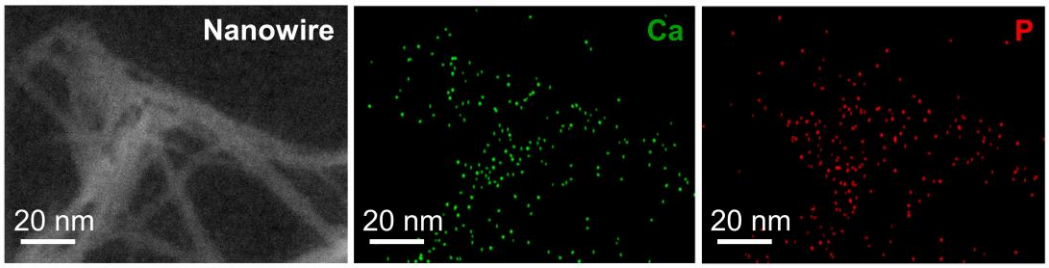

Supplementary Fig. 13. STEM (left) image and EDS (middle and right) elemental mapping of ACP nanowires.

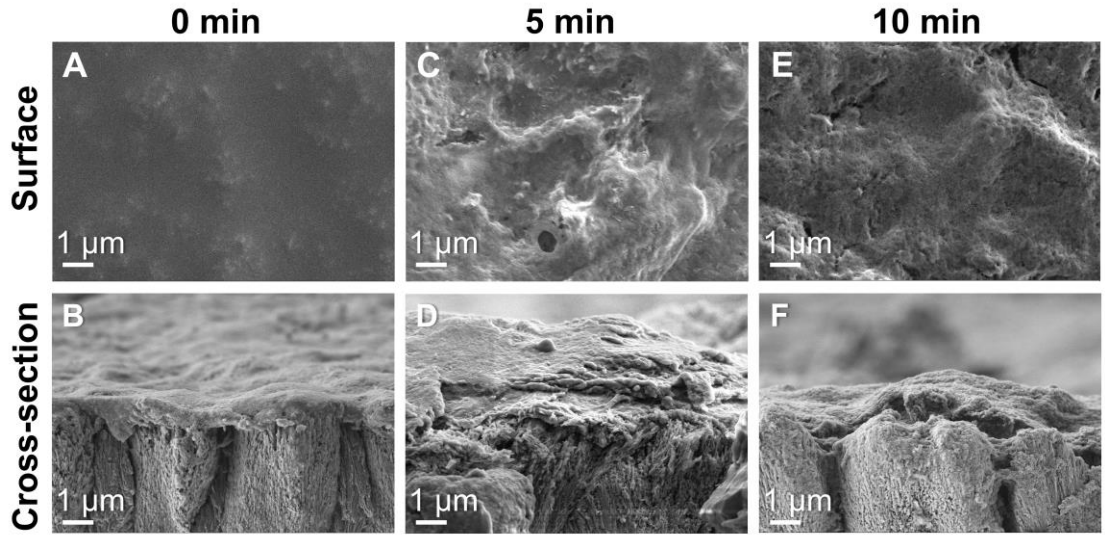

Supplementary Fig. 14. Top and cross-sectional SEM images of the acid etched enamel repaired by GCPC at 0 (A, B), 5 (C, D), 10 min (E, F). The samples after GCPC treatments are gently immersed in ethanol (instead of flushing) to quench the reactions.

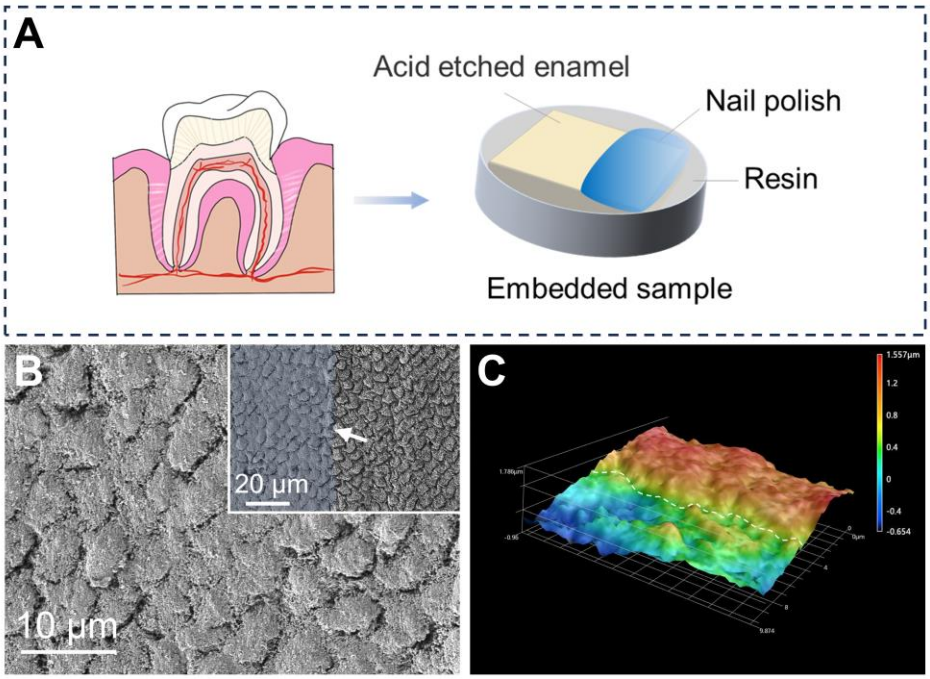

Supplementary Fig. 15. In vitro experiments on enamel blocks. (A) Scheme of the enamel block embedded in resin. After being etched by 37 wt% phosphoric acid, half surface of the enamel is coated with nail varnish as the non-treatment area, and the remaining half is the X treatment area (X: the applied material, e.g., GCPC, CPP-ACP paste). (B) SEM images of the top surface of etched enamel after GCPC treatment for 30 min. The boundary between GCPC treatment area (blue region) and GCPC non-treatment area on enamel is marked by an arrow in inset of (B). (C) 3D laser scanning microscope image of the etched enamel surfaces after repair for 30 min. The non-treatment area shows lower height and the GCPC-treatment area exhibits higher height, where the boundary between the two areas is marked by a dashed line.

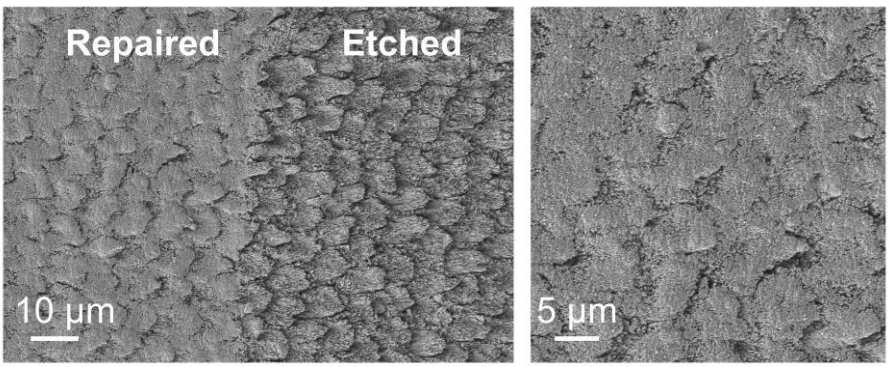

Supplementary Fig. 16. SEM images of enamel repaired by GCPC at 30 min after ultrasonic treatment. The right picture is a high magnification image of the repaired area on the left image.

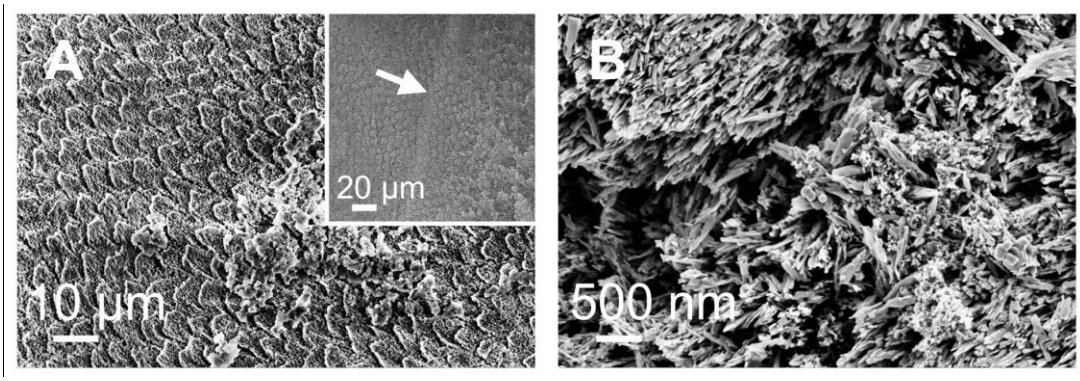

Supplementary Fig. 17. SEM images of the etched enamel repaired by CPP-ACP paste for 30 min. The repaired enamel surfaces appear in low (A) and high (B) magnifications. The boundary between the CPP-ACP paste treatment and non-treatment areas is marked with an arrow in inset of (A).

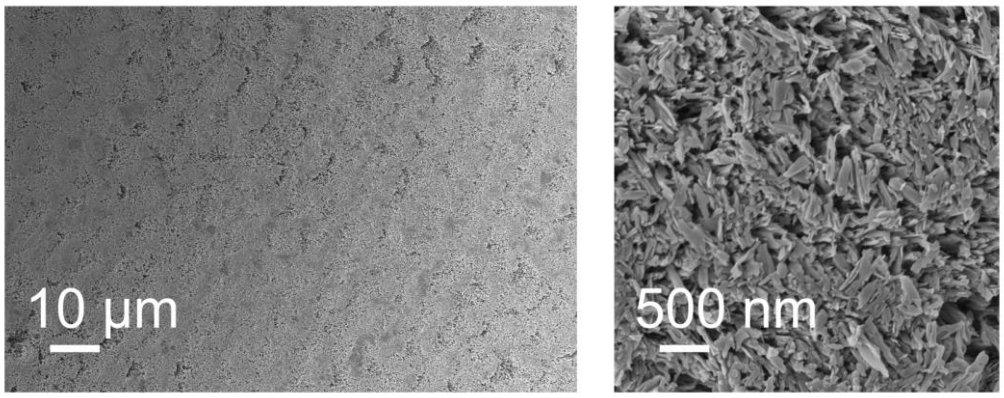

Supplementary Fig. 18. SEM images of the etched enamel repaired by 3X-GCPC for 30 min.

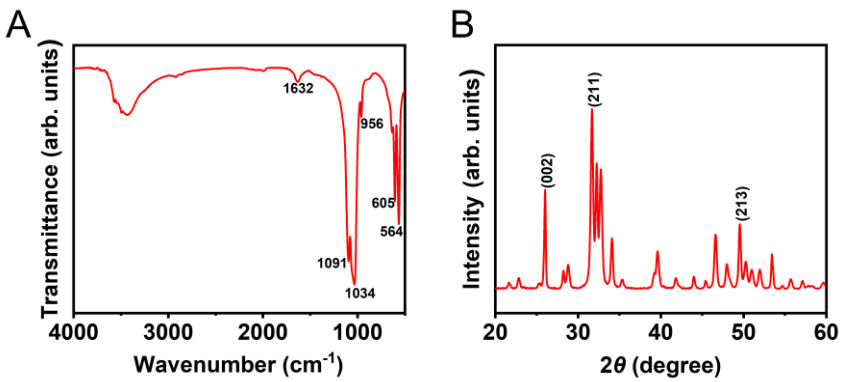

Supplementary Fig. 19. FTIR spectrum (A) and XRD pattern (B) of the synthesized HAP nanorod.

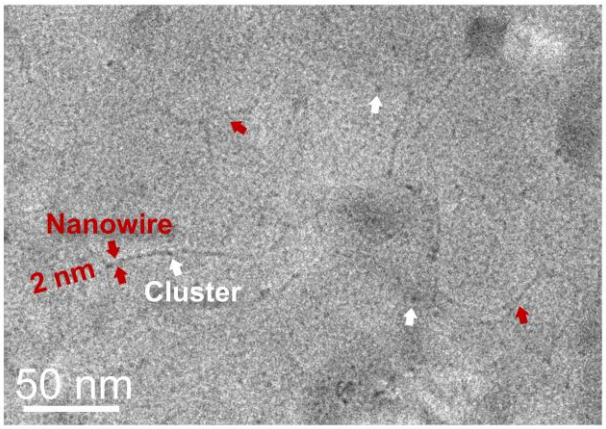

Supplementary Fig. 20. Cryo-TEM image of nanowires formed in artificial saliva at 3 min. The red and white arrows indicate nanowires and cluster, respectively.

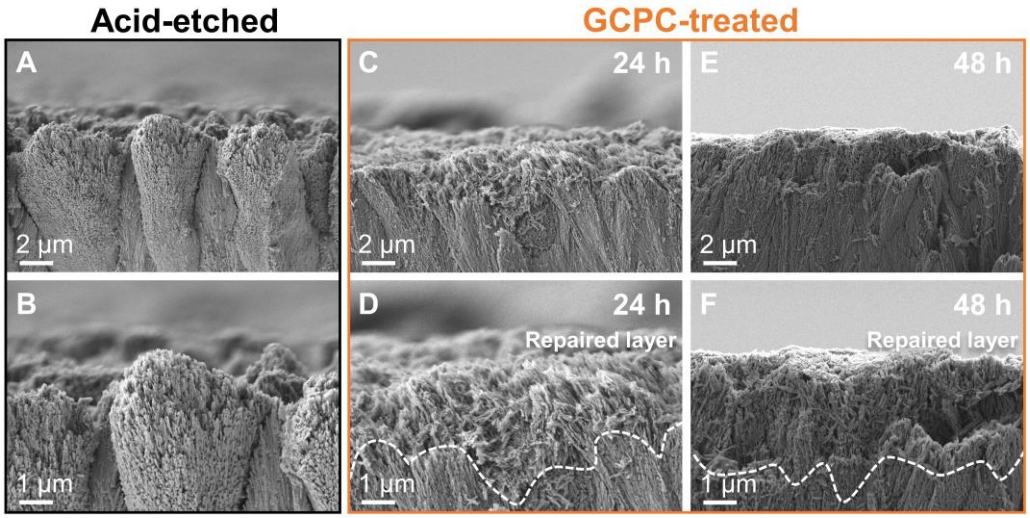

Supplementary Fig. 21. Cross-sectional SEM images of etched enamel repaired by GCPC for 24 h and 48 h. (A, B) The acid-etched enamel surface. (C-F) Enamel surfaces treated by GCPC for 24h (C, D) and 48h (E, F). The dashed line in each image indicates the boundary between the speculated repair layer and the natural enamel.

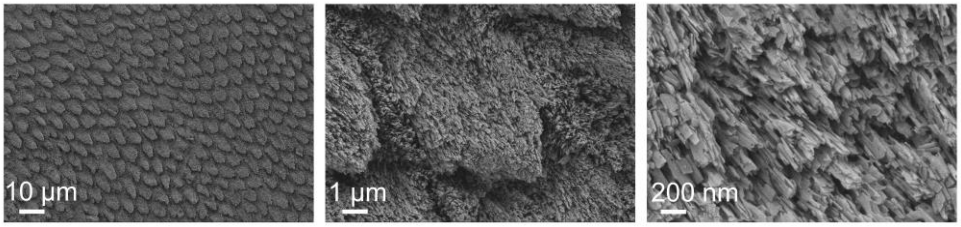

Supplementary Fig. 22. SEM images of the etched enamel after being incubated in artificial saliva (without treatment by repair materials) for 24 h.

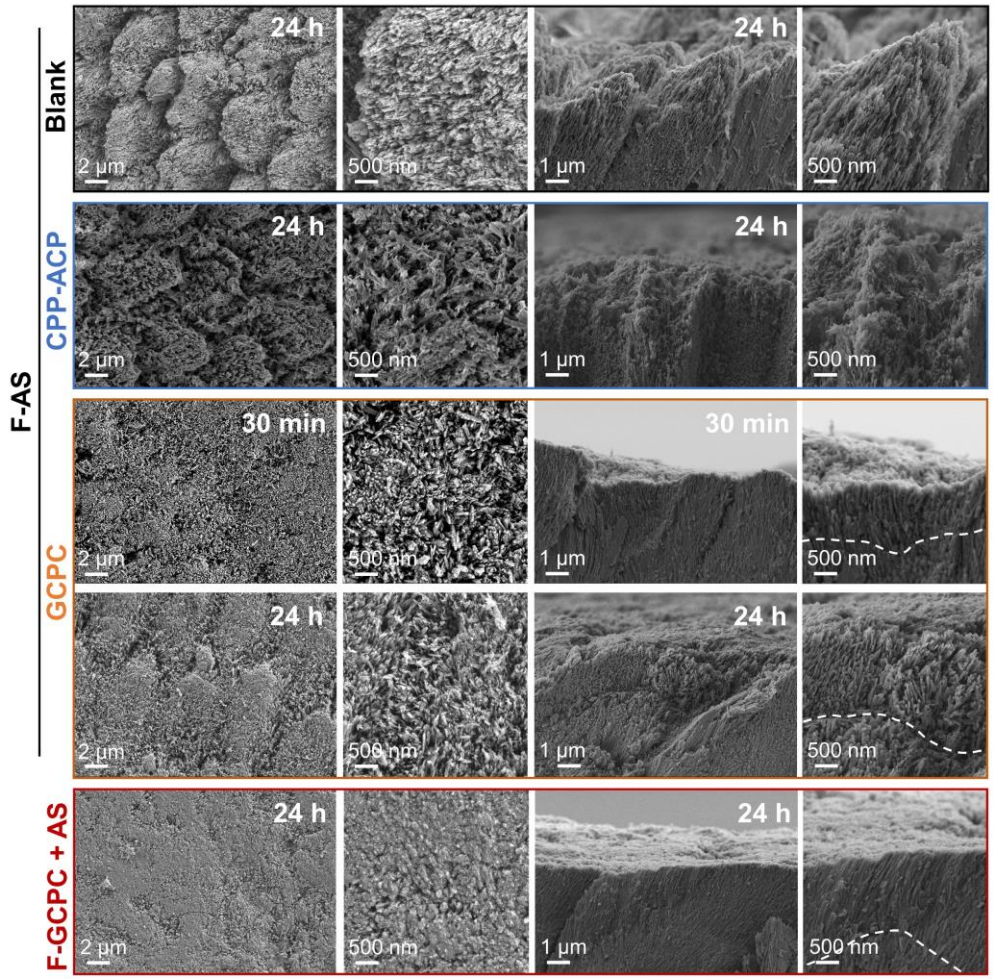

Supplementary Fig. 23. SEM images from the top surface and cross-sectional view of etched enamel without any treatment (Blank, 1st row) or with a treatment (2nd to 4th rows) as indicated. The incubation of the samples treated with CPP-ACP and GCPC are in fluorine-containing artificial saliva (F-AS), while those with fluorine-containing GCPC (F-GCPC) are in normal artificial saliva (AS) for the time as indicated on the figure. The dashed lines indicate the speculated boundary between the repair layer and the natural enamel.

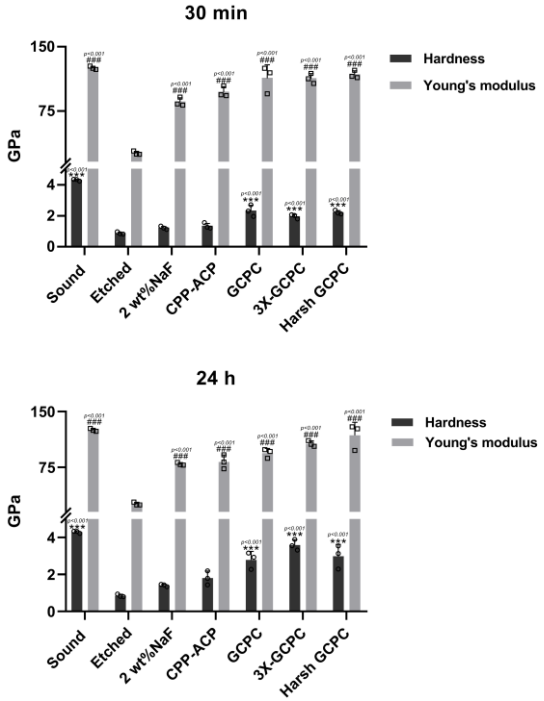

Supplementary Fig. 24. Hardness and Young's modulus of different enamel samples after repair for 30 min and 24 h determined by nanoindentation. Sound, etched, 2 wt% NaF, CPP-ACP, GCPC, and 3X-GCPC correspond to the samples of sound enamel, etched enamel (blank group), enamels repaired by 2 wt% NaF, CPP-ACP paste, GCPC and 3X-GCPC in static artificial saliva respectively; Harsh GCPC represents the enamel repaired by GCPC under oscillation condition. The asterisk (*) and hashtag ($^{\#}$) denote significant differences of hardness and Young's modulus respectively between the indicated group and the etched group. The error bars represent the mean ± SD for n = 3 independent experiments, * or $^{\#}p < 0.05$, ** or $^{\#\#}p < 0.01$, *** or $^{\#\#\#}p < 0.001$; no data were excluded from the analyses.

Compared with sound enamel with a hardness of 4.29 ± 0.07 GPa and Young's modulus of 125.18 ± 1.92 GPa, acid etching treatment results in significantly reduced hardness (0.85 ± 0.079 GPa) and Young's modulus (25.80 ± 2.20 GPa). After GCPC treatment for 30 min, the newly formed HAP crystals exhibit noticeably enhanced hardness 2.30 ± 0.38 GPa (Young's modulus:113.11 ± 15.86 Gpa), and that of the repaired enamel by 3X-GCPC and GCPC in oscillator (Harsh GCPC) increases to 1.94 ± 0.14 GPa (Young's modulus:112.83 ± 5.79 GPa) and 2.20 ± 0.13 GPa (Young's modulus:117.35 ± 4.51 GPa), respectively. The hardness of the repaired enamel is further increased after incubation for 24 h, reaching the values of 2.79 ± 0.46 Gpa (GCPC), 3.59 ± 0.29 GPa (3X GCPC) and 2.99 ± 0.64 GPa (Harsh GCPC), possibly due to ripening process of crystals. However, no significant difference of hardness is found in both 2 wt% NaF and CPP-ACP paste groups compared with that acid etched enamel at either 30 min or 24 h, although the Young' s modulus in these group are improved. The above results are consistent with the conclusions by Vickers-hardness test in manuscript, i.e.no matter in the static and oscillated environments, GCPC treatment recovers the mechanical properties to the values close to that of natural enamel, and whose performance better than the conventional remineralization materials/commodities, e.g., 2 wt% NaF and CPP-ACP.

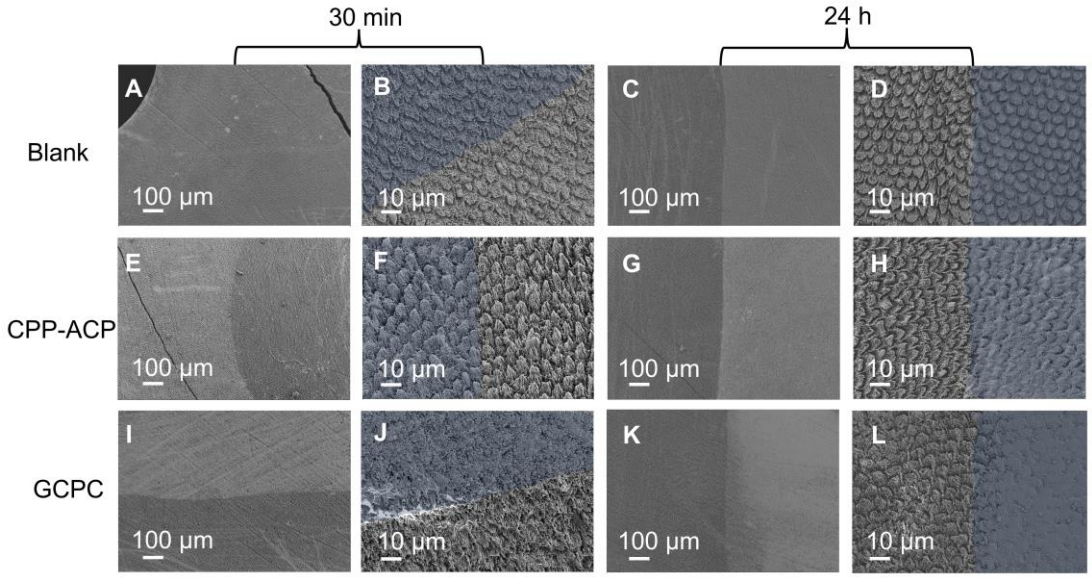

Supplementary Fig. 25. SEM images of the acid etched enamels after being treated with different materials (deionized water, CPP-ACP paste, GCPC) in vivo for 30 and 24 h. (A-D) Enamels treated with deionized water (Blank). (E-H) Enamels treated with CPP-ACP. (I-L) Enamels treated with GCPC. Blue regions: the material treatment areas.

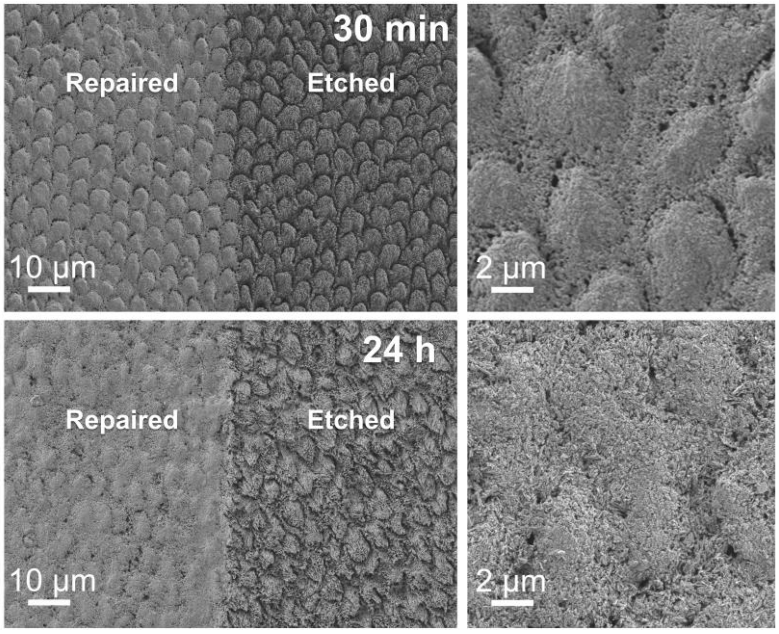

Supplementary Fig. 26. SEM images of enamel repaired by GCPC in animal study at 30 min and 24 h after ultrasonic treatment. The right one is a high magnification image of the repaired area on the left one.

Supplementary Table 1. Comparison of GCPC with the representative materials explored for enamel remineralization in the past 15 years. AS: artificial saliva, SBF: simulated body fluid, Glu: glutamic acid, MMP-20: matrix metalloproteinase-20, CS-AMEL: hydrogel system composed of chitosan-amelogenin, PCBAA: zwitterionic poly-(carboxybetaine acrylamide).

Year	Repair materials	Pre-treatment (before immersed in AS /SBF)	Time for significant remineralization in vitro*	Thickness of the repaired layers
2011[1]	Glu-Directed assembly of apatite nanoparticles	Coat the material on enamel, then wash with ethanol and dry in air at 25 ºC	72 h, the particles turned into rod-like apatite crystals	0.6~1μm in 3d
2017[2]	Chimaeric-peptide-guided ACP nanoparticles	Coat the material on enamel, then brush for 10 min	7 d, a layer of ordered enamel-like crystals was formed	No data
2018[3]	MMP-20/CS-AMEL hydrogel	Coat the material on enamel, then keep in a desiccator for 15 min	5 d, needle-like HAP crystals were formed	No data
2019[4]	Calcium phosphate ion clusters	Coat the material on enamel, then dry in air for 15 min	48 h, the coated material formed a well-crystallized HAP layer	2.0~2.8μm
2020[5]	Amyloid-like amelogenin mimics	Immerse the enamel in the solution containing the material for 10 min	7 d, a layer of the rod-like HAP crystals was formed	2.0~2.8μm
2021[6]	Biomimetic enamel matrix proteins	Coat the material on enamel, crosslink it, then dry in air	24 h, the prismatic and interprismatic structures were restored with newly formed HAP crystals	2 μm
2022[7]	Low-complexity protein segments	Immerse the enamel in a solution containing the material for 12 h, then wash with water and dry in air	3 d, initial formation of a new HAP layer	4.6 and 5.1μm in 6 d
2022[8]	PCBAA/ACP nanocomposite	Coat the enamel with fresh material	1 d, interprismatic	10.5 μm in 7 d

			zones were almost filled with the newly formed HAP crystals	
2022[9]	Lysozyme conjugated with poly (ethylene glycol)	Immerse the enamel in a solution containing the material, then apply pressure for 5 to 10 min and dry in air	2 d, a dense, well-organized, newly formed HAP layer was observed	17.5 μm in 14 d
2023[10]	Ribonucleic acid-stabilized amorphous calcium phosphate (RNA-ACP) and ribonuclease (RNase)	Coat the enamel with RNA-ACP nanocomposite, and immerse in artificial saliva containing RNase A	1d, the epitaxial growth of dense and well-oriented rod-like crystals was confirmed	3-5 μm in 1 d
2023[11]	Peptide amphiphile (PA)	Immerse the enamel in a solution containing PA	Newly formed HAP crystals were tightly packed, contributing to a denser structure than that resulting from acid etching	1.5 μm in 3 d
This work	GCPC	Brush the enamel for 5 s during material coating	30 min, the coated material completely transformed into compact HAP nanorods	3 μm in 2 d

*: Here we present the earliest time points when the adsorbed materials on the enamels completely transformed into apatite crystals, or induced the formation of apatite crystals.

Reference

[1] L. Li, C. Mao, J. Wang, X. Xu, H. Pan, Y. Deng, X. Gu, R. Tang. **Bio-inspired enamel repair via Glu-directed assembly of apatite nanoparticles: an approach to biomaterials with optimal characteristics**. *Adv. Mater.* **2011**, *23*, 4695-4701. 10.1002/adma.201102773.

[2] Z. Xiao, K. Que, H. Wang, R. An, Z. Chen, Z. Qiu, M. Lin, J. Song, J. Yang, D. Lu, M. Shen, B. Guan, Y. Wang, X. Deng, X. Yang, Q. Cai, J. Deng, L. Ma, X. Zhang, X. Zhang. **Rapid biomimetic remineralization of the demineralized enamel surface using nano-particles of amorphous calcium phosphate guided by chimaeric peptides**. *Dent. Mater.* **2017**, *33*, 1217-1228. 10.1016/j.dental.2017.07.015.

[3] S. Prajapati, Q. Ruan, K. Mukherjee, S. Nutt, J. Moradian-Oldak. **The Presence of MMP-20 Reinforces Biomimetic Enamel Regrowth**. *J. Dent. Res.* **2018**, *97*, 84-90. 10.1177/0022034517728504.

[4] C. Shao, B. Jin, Z. Mu, H. Lu, Y. Zhao, Z. Wu, L. Yan, Z. Zhang, Y. Zhou, H. Pan, Z. Liu, R. Tang. **Repair of tooth enamel by a biomimetic mineralization frontier ensuring epitaxial growth**. *Sci. Adv.* **2019**, *5*, eaaw9569. 10.1126/sciadv.aaw9569.

[5] D. Wang, J. Deng, X. Deng, C. Fang, X. Zhang, P. Yang. **Controlling Enamel Remineralization by Amyloid-Like Amelogenin Mimics**. *Adv. Mater.* **2020**, *32*, 2002080. 10.1002/adma.202002080.

[6] Z. Fang, M. Guo, Q. Zhou, Q. Li, H. M. Wong, C. Y. Cao. **Enamel-like tissue regeneration by using biomimetic enamel matrix proteins**. *Int. J. Biol. Macromol.* **2021**, *183*, 2131-2141. 10.1016/j.ijbiomac.2021.06.028.

[7] R. Chang, Y. J. Liu, Y. L. Zhang, S. Y. Zhang, B. B. Han, F. Chen, Y. X. Chen. **Phosphorylated and Phosphonated Low-Complexity Protein Segments for Biomimetic Mineralization and Repair of Tooth Enamel**. *Adv. Sci.* **2022**, *9*, 2103829. 10.1002/advs.202103829.

[8] J. He, J. Yang, M. Li, Y. Li, Y. Pang, J. Deng, X. Zhang, W. Liu. **Polyzwitterion Manipulates Remineralization and Antibiofilm Functions against Dental Demineralization**. *ACS Nano* **2022**, *16*, 3119–3134. 10.1021/acsnano.1c10812.

[9] X. Yang, J. Guo, B. Hu, Z. Li, M. Wu, H. Guo, X. Huang, X. Liu, X. Guo, P. Liu, Y. Chen, S. Li, Y. Gu, H. Wu, K. Xuan, P. Yang. **Amyloid-Mediated Remineralization in Pit and Fissure for Caries Preventive Therapy**. *Adv. Healthcare Mater.* **2022**, *11*, 2200872. 10.1002/adhm.202200872.

[10] C. Lei, K.-y. Wang, Y.-x. Ma, D.-x. Hao, Y.-n. Zhu, Q.-q. Wan, J.-s. Zhang, F. R. Tay, Z. Mu, L.-n. Niu. **Biomimetic Self-Maturation Mineralization System for Enamel Repair**. *Adv. Mater.* **2024**, *9*, 2311659. 10.1002/adma.202311659.

[11] Z. Tang, Z. Chen, D. Wang, S. Shan, W. Jin, K. Sun, H. Pan, Z. Xie, R. Tang, C. Shao. **Peptide Amphiphile-Mediated Assembly and Fusion of Anisotropic Amorphous Particles for Enamel Remineralization**. *Adv. Funct. Mater.* **2024**, *34*, 2306900. 10.1002/adfm.202306900.